Supporting information for

Effect of Pressure on Interband and Intraband Transition of Mercury Chalcogenides Quantum Dots

Clément Livache[1,2], Nicolas Goubet[1,2], Charlie Gréboval[1], Bertille Martinez[1,2], Julien Ramade[1], Junling Qu[1], Amaury Triboulin[1], Hervé Cruguel[1], Benoit Baptiste[3], Stefan Klotz[3], Guy Fishman[4], Sébastien Sauvage[4], Francesco Capitani[5], Emmanuel Lhuillier[1*]

[1]Sorbonne Université, CNRS, Institut des NanoSciences de Paris, INSP, F-75005 Paris, France

[2]Laboratoire de Physique et d'Etude des Matériaux, ESPCI-ParisTech, PSL Research University, Sorbonne Université UPMC Univ Paris 06, CNRS, 10 rue Vauquelin 75005 Paris, France.

[3]Sorbonne Université, CNRS, Institut de Minéralogie, de Physique des Matériaux et de Cosmochimie, IMPMC, F-75005 Paris, France

[4]Centre de Nanosciences et de Nanotechnologies, CNRS, Univ. Paris-Sud, Université Paris-Saclay, C2N – 10 boulevard Thomas Gobert, 91460 Palaiseau, France

[5]Synchrotron-SOLEIL, Saint-Aubin, BP48, F91192 Gif sur Yvette Cedex, France

To whom correspondence should be sent: el@insp.upmc.fr

Table of content
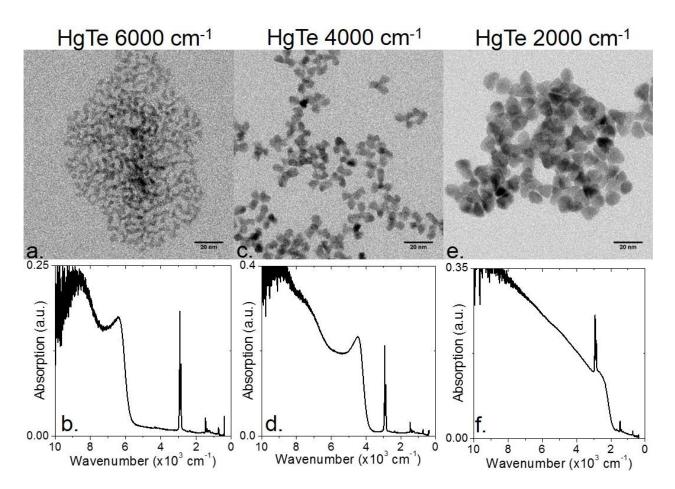
1. HgTe CQD synthesis

Figure S 1a and b are respectively TEM image and zero pressure infrared spectrum from HgTe CQD with a band edge energy at 6000 cm^{-1}. c and d are respectively TEM image and zero pressure infrared spectrum from HgTe CQD with a band edge energy at 4000 cm^{-1}. e and f are respectively TEM image and zero pressure infrared spectrum from HgTe CQD with a band edge energy at 2000 cm^{-1}
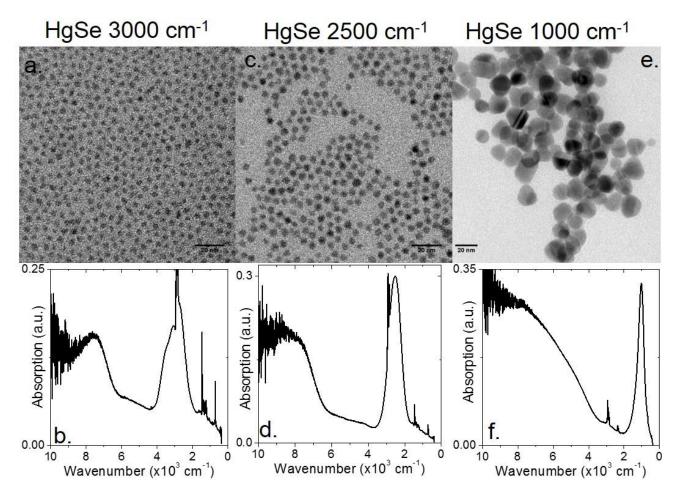
2. HgSe CQD synthesis

Figure S 2a and b are respectively TEM image and zero pressure infrared spectrum from HgSe CQD with an intraband peak energy at 3000 cm^{-1}. c and d respectively TEM image and zero pressure infrared spectrum from HgSe CQD with an intraband peak energy at 2500 cm^{-1}. e and f respectively TEM image and zero pressure infrared spectrum from HgSe CQD with an intraband peak energy at 1000 cm^{-1}

3. Material characterization

Under high pressure, the zinc blende phase of the HgTe nanocrystal switches toward a cinnabar phase, which refined diffractogram is provided in Figure S 3a. A scheme of the cinnabar HgTe unit cell is given in Figure S 3b. We found the structural parameter of the hexagonal phase of HgTe to be a=b=0.447 nm and c=0.943 nm under 5.5 GPa of pressure.
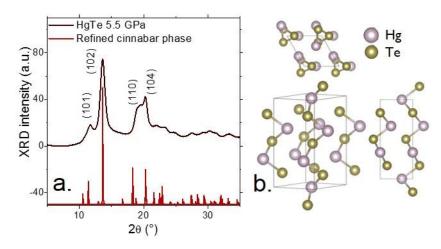

Figure S 3 a. Experimental and refined X-ray diffractogram from HgTe nanocrystal under a 5.5 GPa pressure. b. Scheme of the HgTe cinnabar unit cell.

4. IR spectroscopy under pressure

4.1. Signal filtering

The infrared data obtained from the setup described in figure 2 of the main text present oscillations, see Figure S 4. They result from interference with the diamond cell. The high frequency oscillations are then removed using an FFT filtering procedure, see Figure S 4.
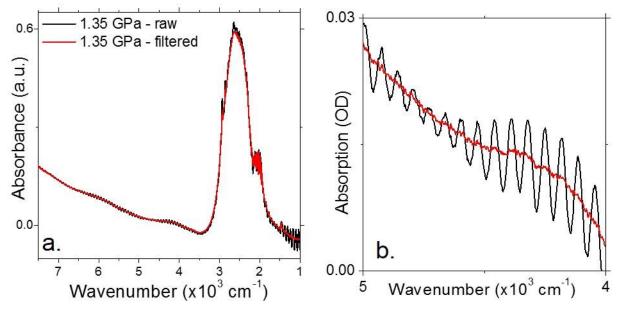

Figure S 4 a raw and filtered infrared spectrum obtained from HgSe CQD with intraband peak energy at 2500 cm^{-1}. b is a zoom on the same spectrum in the range of energy between 4000 and 5000 cm^{-1}.

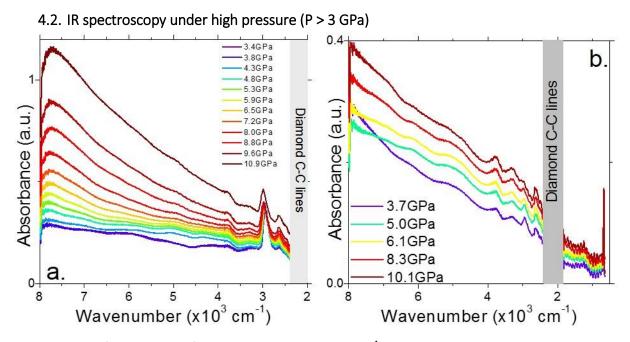## 4.2. IR spectroscopy under high pressure (P > 3 GPa)

Figure S 5 a. Infrared spectra for HgTe CQD, with a 6000 cm^{-1} band edge at zero pressure, in the 3 to 10 GPa range of pressure. b Infrared spectra for HgSe CQD, with a 1000 cm^{-1} intraband peak at zero pressure, in the 3 to 10 GPa range of pressure.

5. k·p simulation

The energy dispersion $E(k)$ with wavevector k in the Brillouin zone is calculated using a Pidgeon-Brown 8 band **k.p** formalism as show in Figure S 6a.[1] The bulk states at the **k** vector are developed on a limited set consisting in 8 zone center Bloch states of Γ_6, Γ_7 and Γ_8 symmetry. Through adjustable parameters the 8x8 matrix accounts for the **k.p** interaction between these states but also for the perturbative influence of the zone center states outside of the basis set. These **k.p** parameters are chosen to reproduce as closely as possible the band structure given in the figure 3(c) from Ref. [2] obtained through the h-QSGW scheme of Svane *et al*. Note that on purpose we do not introduce the linear term in the **k.p** matrix that leads to the splitting of the heavy Γ_8 band along $\Gamma - L$ obtained by Svane *et al* since this splitting plays a negligible contribution to the interband energy. The obtained **k.p** dispersions $E(k)$ of the 8 bands are given Figure S 6a. It is plotted using the same scale as Ref [2] in order to be readily compared.

The dispersion of the two Γ_8 bands can be approximated near the Brillouin zone center through the Dresselhaus-Kip-Kittel formula[3] $E(k) = E(k = 0) + Ak^2 \pm \sqrt{B^2 k^4 + C^2\left(k_x^2 k_y^2 + k_y^2 k_z^2 + k_z^2 k_x^2\right)}$, with A=37.8 $\hbar^2/2/m_0$, B=-20.39 $\hbar^2/2/m_0$, C=-107.8 $\hbar^2/2/m_0$ obtained from the **k.p** hamiltonian. $\hbar = h/2/\pi$ is the reduced Plank constant and m_0 is the electron mass. This formula amounts to a parabolic dispersion along each direction of the Brillouin zone. We use this parabolic dispersion to evidence the strong non parabolicity of $E(k)$ a few percent away from the Brillouin zone in the comparison of Figure 5a.

In semiconductors exhibiting a cubic structure, a hydrostatic pressure P produces a scalar deformation tensor ϵ so that for the diagonal elements $\epsilon_{xx} = \epsilon_{yy} = \epsilon_{zz} = P/3/B$ where B is the bulk modulus and $\epsilon_{xy} = \epsilon_{yz} = \epsilon_{zx} = 0$ for the shear strain component.[4] Since the contraction of the lattice parameter produces an expansion of the Brillouin zone and simultaneously an expansion of the wavevectors k involved in the confined states, we neglect these two roughly self-cancelling effects in the strained electronic structure calculations. The effect on strain on the energy dispersion is accounted for through the change in the energy difference between Γ_6 and Γ_8 state energies at the zone center with a deformation potential of $d(E_{\Gamma_6} - E_{\Gamma_8})/d\epsilon/3$ =-2.4 eV. As depicted in Figure S 6b and 5a, the pressure first results in a decrease of the conduction band effective mass $m_e^*(k = 0, P)$, until $\epsilon = -2.2\%$ where the band gap opens and the effective mass increases again. The equivalent mass $m_e^*(k, P)$ calculated at $k = 10\%$ $2\pi/a$ along the $\Gamma - L$ direction follows the same trend but with much less amplitude variation.
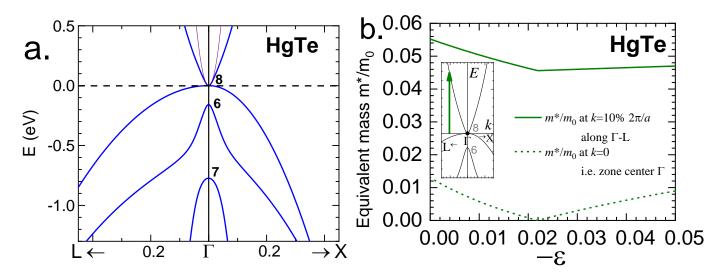

*Figure S 6 Simulated band structure of HgTe at zero strain from **k·p** simulation. Parameters are obtained by fitting the predicted band structure by Svane et al.[2] . b. Equivalent mass of the conduction band as a function of strain ϵ, at the zone center and at 10% of the Brillouin zone along $\Gamma - L$. The equivalent mass is the mass m^* that gives the energy E of the conduction band at **k** point through the formula $E = E(k = 0) + \frac{\hbar^2 k^2}{2m^*}$.*

6. References

(1) Pidgeon, C. R.; Brown, R. N. *Phys. Rev.* **1966**, *146*, 575–583.

(2) Svane, A.; Christensen, N. E.; Cardona, M.; Chantis, A. N.; van Schilfgaarde, M.; Kotani, T. *Phys. Rev. B* **2011**, *84*, 205205.

(3) Dresselhaus, G.; Kip, A. F.; Kittel, C. *Phys. Rev.* **1955**, *98*, 368–384.

(4) YU, P.; Cardona, M. *Fundamentals of Semiconductors: Physics and Materials Properties*, 4th ed.; Graduate Texts in Physics; Springer-Verlag: Berlin Heidelberg, 2010.